Monatshefte für Chemie 135, 1047–1059 (2004)
DOI 10.1007/s00706-004-0173-y

Monatshefte für Chemie
Chemical Monthly
Printed in Austria

Systematic Investigation of Non-Nucleoside Inhibitors of HIV-1 Reverse Transcriptase (NNRTIs)

Anton Beyer[1,*], **Luckhana Lawtrakul**[2,*], **Supa Hannongbua**[3], and **Peter Wolschann**[4]

[1] Research Institute of Molecular Pathology, 1030 Vienna, Austria
[2] Department of Common and Graduate Studies, Sirindhorn International Institute of Technology (SIIT), Thammasat University, P.O. Box 22 Thammasat Rangsit Post Office, Pathumthani 12121, Thailand
[3] Department of Chemistry, Faculty of Science, Kasetsart University, Bangkok 10900, Thailand
[4] Institute of Theoretical Chemistry and Structural Biology, 1090 Vienna, Austria

Received December 29, 2003; accepted January 15, 2004
Published online April 26, 2004

Summary. The 44 crystal structures of NNRTIs complexed with HIV-1 reverse transcriptase (RT) have been analyzed in detail especially the orientation geometries and the distances between inhibitor molecules and surrounding amino acids. In general, various NNIs bind to the same region of the HIV-1 RT in the palm subdomain of p66, but subtle differences in individual interactions between RT and its inhibitors can be detected by comparison of all structures in this study.

Keywords. Non-nucleoside reverse transcriptase inhibitors (NNRTIs); Inhibition mechanism; Viral mutation; Drug resistance.

Introduction

In recent years, a major challenge facing medicinal chemistry is the development of drugs with significantly improved resistance profiles for chronic use as anti-HIV combination therapy [1]. An important component of this regimen is non-nucleoside HIV-1 reverse transcriptase inhibitors (NNRTIs). The NNRTIs interact non-competitively with an allosteric site of the enzyme and thus do not directly impair the function of the substrate's binding site [2]. Their interaction with HIV-1 RT leads to a conformational change in the enzyme, resulting in a decrease in the affinity of the active site for the substrate, which we present in our previous

* Corresponding authors. E-mails: beyer@nt.imp.univie.ac.at; luckhana@siit.tu.ac.th

publication [3]. NNRTIs are a class of structurally diverse aromatic compounds. They can be put into the following categories: 1) Hydroxyethoxymethylphenylthiothymine (*HEPT*) derivatives [4], 2) Tetrahydroimidazobenzodiazepinone (*TIBO*) derivatives [5], 3) Dihydropyridodiazepinone such as nevirapine derivatives [6], 4) Pyridinone derivatives [7], 5) Bis(heteroaryl)piperazine (*BHAP*) derivatives [8], 6) Tertiarbutyldimethylsilylspiroaminooxathioledioxide (*TSAO*) pyrimidine nucleosides [9], and 7) α-Anilinophenylacetamide (α-*APA*) derivatives [10]. In general, various non-nucleoside inhibitors (NNIs) bind to the same region of the HIV-1 RT in the palm subdomain of p66, but subtle differences in individual interactions between RT and its inhibitors can been detected by the comparison of all structures in this study. Many, but not all NNIs possess a butterfly-like shape with two hydrophobic wings connected by a polar central body. We present here the calculation of the dihedral angles for all structures, which allows us to determine quantitative structural changes of HIV-1 RT on binding to NNIs or to *RNA/DNA*. All reported NNRTI-resistant mutations occur in residues surrounding the inhibitor-binding site of the enzyme [2]. A commonly observed drug resistance is one for which important interactions of the aromatic moiety of the inhibitors and the neighboring residues *Tyr*181, *Tyr*188, *Phe*227, and *Trp*229 are lost. Additionally a *Lys*103*Asn* mutation appears relatively frequently giving resistance to many NNRTIs [11]. For a complete understanding of the inhibition mechanism of HIV-1 RT the detailed knowledge of the conformations of the amino acid residues involved is necessary. To this end the determination of more structures will be necessary, especially of mutant type enzyme complexes.

Results and Discussion

NNI Binding to RT

All NNIs where the structure of the RT complex is currently known, bind to a region of the enzyme, which is approximately 10 Å away from the catalytic site [12, 13]. This region, which is called NNI binding pocket, forms a cavity and is located between two sheets β4, β7, β8 of the fingers domain and β9, β10, β11 of the p66 palm domain. It also includes the β5–β6 loop (*Pro*97, *Leu*100, *Lys*101, *Lys*103), β6 (*Ser*105, *Val*106, *Val*108), the β9–β10 hairpin (*Val*179, *Tyr*181, *Tyr*188, *Gly*190, *Asp*192), the β12–β13 hairpin (*Glu*224, *Phe*227, *Trp*229, *Leu*234, *Pro*236) and part of β15 (*Tyr*318, *Tyr*319) [14] (see also Fig. 2 in Ref. [3] for details). The internal surface of the pocket is predominantly hydrophobic with substantial aromatic character (*Tyr*181, *Tyr*188, *Phe*227, *Trp*229, *Tyr*232). In addition it includes few hydrophilic residues (*Lys*101, *Lys*103, *Ser*105, *Asp*192, *Glu*224) and backbone atoms, which are suitable to form hydrogen bonds with the inhibitor. A small part of the pocket is formed by amino acid residues from the p51 subunit (*Thr*135, *Glu*138). There is no NNI binding pocket in p51 itself. A solvent accessible entrance to the cavity is formed by several residues from p66 (*Leu*100, *Lys*103, *Val*179, *Ser*191) and *Glu*138 from p51. The interactions between four selected NNIs and the surrounding amino acid residues are depicted in Fig. 1.

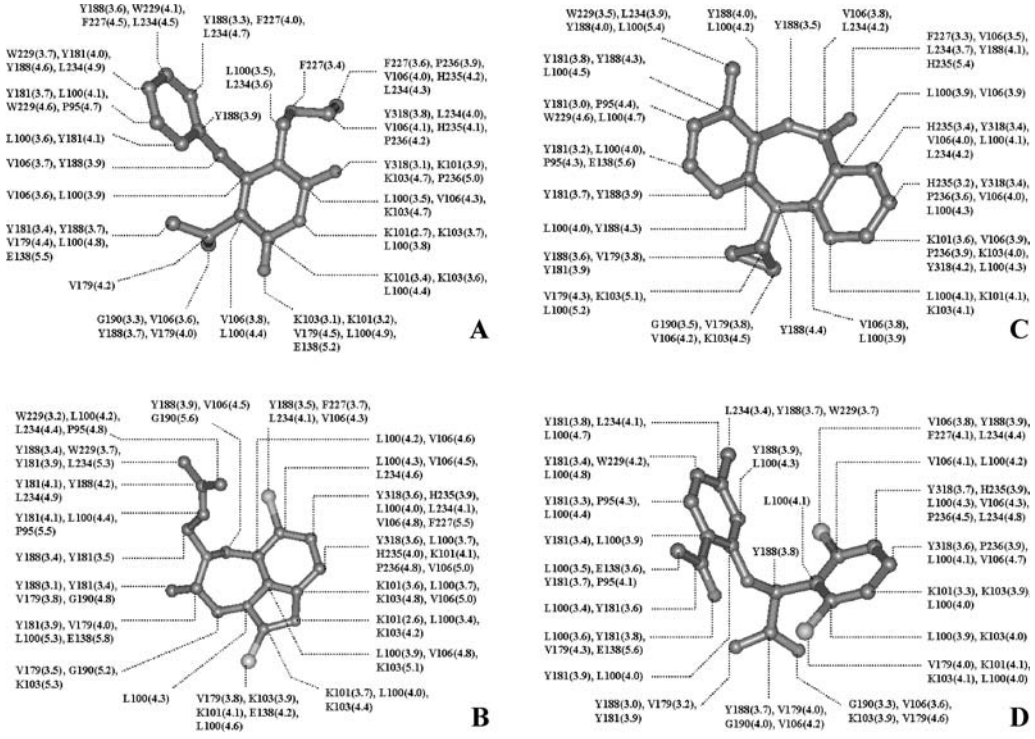

Fig. 1. Schematic diagrams showing the intermolecular interactions between NNIs and surrounding amino acid residues of HIV-1 RT within an interatomic distance of 6 Å, *HEPT*; 8-Cl *TIBO*; Nevirapine; 2,6-Cl_2 α-*APA*

The list of Table 1 shows residues of RT, which have distances less than 4 Å to the inhibitor calculated for all available structures. This table helps to identify important residues for inhibitor binding and also shows clearly the differences between various inhibitors. The importance of residues *Leu*100, *Lys*101 and of the aromatic residues *Tyr*181, *Tyr*188, *Trp*229, and *Tyr*318 is easily recognized. These residues are in close contact with every inhibitor. For the amino acid residues listed in Table 1 and for residues forming the polymerase active site of RT, backbone and side chain dihedral angles have been calculated for all available structures. Table 2 is a subset of this list showing the dihedral angles of eight important residues (*Tyr*181, *Tyr*188, *Trp*229, *Pro*236 from the NNI binding pocket and *Asp*110, *Met*184, *Asp*185, *Asp*186 from the active site) from nine structures. This table allows a closer examination of the differences between various structures. Some examples will be discussed later on in more detail.

Superposition of four structures was performed using the backbone atoms of the residues mentioned in Table 1 as scaffold. This procedure leads to a pharmacophoric overlay of the NNIs, showing a butterfly-like shape with two hydrophobic wings connected by a polar central body as shown in Fig. 2. In general NNIs consist of two hydrophobic moieties (wing I and wing II) connected by a linker group [15]. The two hydrophobic wings, aromatic rings in most cases, have strong interactions with the aromatic side chains of the NNI binding pocket (Fig. 2).

Table 1. Amino acid residues in contact with NNIs within a distance of <4 Å

Mutation[a]	1RTI	1RT1	1RT2	1JLA1	1C1B	1C1C	1JLQ	1HNV	1UWB1	1TVR	1REV	3HVT	1VRT	1FKP2	1JLB1	1JLF3	1RTH	1RT34	1VRU	1HPZ2	1HNI	1BQM	1BQN3	1HQU2	1KLM	1RT5	1RT6	1RT7	1RT4	1JLG3	1COT	1COU	1DTT	1JLC3	1DTQ	1EET	1IKY	1IKX	1FK9	1IKW	1FKO2	1IKV2	1JKH1	1EP4
*Pro*95										X	X			X			X	X				X							X	X				X	X	X					
*Leu*100	X	X	X	X	X	X	X	X	X	X	X	X	X	X	X	X	X	X	X	X	X	X	X	X	X	X	X	X	X	X	X	X	X	X	X	X	X	X	X	X	X	X	X
*Lys*101	X	X	X	X	X	X	X	X	X	X	X	X	X	X	X	X	X	X	X	X	X	X	X	X	X	X	X	X	X	X	X	X	X	X	X	X	X	X	X	X	X	X	X
*Lys*102							X																		X												X						X
*Lys*103	X	X	X	X	X	X	X	X	X	X	X	X		X					X		X			X	X	X	X	X	X	X	X	X	X	X	X	X	X	X	X	X		X	X
*Lys*104																									X																		
*Ser*105			X																																								
*Val*106	X	X	X	X	X	X	X		X	X	X	X	X	X	X	X	X	X	X	X	X	X		X	X	X	X	X	X	X	X	X	X	X	X	X	X	X	X	X	X	X	X	X
*Thr*107																					X																						
*Val*179	X	X	X				X	X		X	X		X	X	X	X	X	X	X	X	X	X	X	X		X	X	X	X	X	X	X	X	X	X	X	X	X	X	X	X	X	X	X
*Ile*180								X		X	X													X							X												
*Tyr*181	X	X	X	X	X	X	X	X	X	X	X	X	X	X	X	X	X	X	X	X	X	X	X	X	X	X	X	X	X	X	X	X	X	X	X	X	X	X	X	X	X	X	X
*Tyr*188	X	X	X	X	X	X	X	X	X	X	X	X	X	X	X	X	X	X	X	X	X	X	X	X	X	X	X	X	X	X	X	X	X	X	X	X	X	X	X	X	X	X	X
*Val*189		X	X	X		X	X							X	X	X			X	X	X	X	X	X			X			X	X					X	X	X	X	X	X
*Gly*190		X	X	X	X	X	X				X	X	X	X	X	X			X	X	X	X	X	X		X		X	X	X	X	X				X	X	X	X	X	X	X
*Glu*224																									X																		
*Pro*225	X	X	X	X		X																X			X											X	X					X
*Pro*226																									X																		
*Phe*227	X	X	X	X	X	X		X	X		X	X	X	X	X	X	X	X				X		X	X		X	X	X	X			X		X	X	X	X	X	X	X	X	X
*Trp*229	X	X	X	X	X	X	X	X	X	X	X	X	X	X	X	X	X	X	X	X	X	X	X	X	X	X	X	X	X		X	X	X		X	X	X	X	X		X	X	X	X
*Leu*234	X	X	X	X	X	X	X			X	X	X	X	X	X		X	X	X	X	X	X	X	X	X	X	X	X	X	X			X	X	X	X	X	X	X	X	X	X	X	X
*His*235	X		X	X	X	X	X	X		X	X		X				X		X		X	X	X	X	X	X		X	X	X			X	X	X	X	X	X	X	X	X	X	X	X
*Pro*236	X	X	X	X	X	X					X	X	X	X			X		X				X		X	X	X		X	X			X	X	X	X	X	X	X	X	X	X	X	X
*Tyr*318	X	X	X	X	X	X	X	X	X	X	X		X	X	X	X	X	X	X	X	X	X	X	X	X	X	X	X	X	X	X	X	X	X	X	X	X	X	X	X	X	X	X	X
*Tyr*319												X																																
*Asn*136[b]																	X																											
*Glu*138[b]							X									X		X	X	X	X					X		X	X		X	X	X	X	X	X					X	

[a] Mutation code: 1 *Tyr*181*Cys*, 2 *Lys*103*Asn*, 3 *Tyr*188*Cys*, 4 *Asp*67*Asn*, *Lys*70*Arg*, *Thr*215*Phe*, *Lys*219*Gln*; [b] Amino acid residues of p51

Table 2. The backbone and the side chain torsion angles (degrees) of some important amino acid residues in the NNI and *dNTP* binding site

[a]	Φ	φ	ω	χ_1	χ_2	χ_3	χ_4
*Tyr*181							
1DLO	−111.8	133.4	179.1	−98.2	87.4	176.8	0.5
1RTD	−74.9	105.4	−180.0	−99.0	74.4	178.1	0.0
1RTI	−121.5	136.0	−179.7	−80.1	44.9	179.0	0.0
1RT1	−118.9	116.4	−179.2	173.4	50.2	−173.3	−0.2
1HNV	−131.4	155.6	179.9	−177.0	81.9	−177.1	0.0
1VRT	−120.6	130.1	−179.8	173.8	66.5	−177.4	−0.2
1VRU	−124.0	124.9	−178.5	171.2	73.4	−170.6	−0.2
1BQM	−143.7	155.9	−178.7	169.2	86.8	−177.6	0.0
1FK9	−111.3	132.4	179.9	168.9	92.3	178.0	−0.1
*Tyr*188							
1DLO	−99.3	129.7	179.4	169.0	96.9	−178.0	−0.2
1RTD	−94.2	108.0	179.6	161.1	107.0	−177.6	0.6
1RTI	−96.7	122.8	−179.4	−65.1	89.2	−179.4	−0.1
1RT1	−99.1	90.6	−179.2	−59.7	79.2	−177.5	−0.4
1HNV	−100.1	104.2	−180.0	−77.1	55.3	−178.6	−0.3
1VRT	−94.9	128.2	−174.7	−69.1	87.2	176.3	0.6
1VRU	−93.8	124.6	−177.4	−62.1	76.3	−179.3	−0.3
1BQM	−89.1	77.4	179.8	−74.3	55.8	178.4	−0.1
1FK9	−82.1	115.2	−179.5	−62.4	79.3	175.3	0.0
*Trp*229							
1DLO	−129.4	109.9	178.8	176.8	61.7	179.6	none
1RTD	−132.0	129.6	177.6	164.9	86.1	179.2	none
1RTI	−113.2	109.9	178.7	−178.1	67.5	−179.8	none
1RT1	−129.2	69.3	179.2	−121.6	45.9	−172.4	none
1HNV	−132.9	129.4	179.5	173.1	85.6	−178.0	none
1VRT	−128.8	131.5	178.7	174.3	86.6	175.0	none
1VRU	−130.8	128.2	178.3	168.5	88.5	178.1	none
1BQM	−97.0	106.7	−178.7	148.5	−115.6	−175.7	none
1FK9	−135.4	126.6	178.4	178.0	76.0	177.9	none
*Pro*236							
1DLO	−45.6	−31.4	−179.3	19.5	−39.4	42.6	none
1RTD	−51.6	−30.3	−179.3	26.9	−44.1	43.8	none
1RTI	−58.9	−26.5	−179.2	29.5	−44.2	41.3	none
1RT1	−54.0	−34.4	−178.9	21.8	−39.8	41.4	none
1HNV	−58.9	−16.5	−179.9	17.6	−31.7	33.3	none
1VRT	−64.4	−29.6	−178	−26.1	40.4	−38.1	none
1VRU	−54.0	−32.6	−175.8	−38.3	45.0	−34.3	none
1BQM	−51.5	3.9	176.7	20.6	−37.9	40.0	none
1FK9	−69.4	−30.0	−178.6	−27.7	42.8	−40.8	none
*Asp*110							
1DLO	−116.8	133.3	−179.9	−163.1	none	none	none
1RTD	−125.1	142.1	180.0	−155.4	none	none	none

(*continued*)

Table 2 (*continued*)

[a]	Φ	φ	ω	χ_1	χ_2	χ_3	χ_4
1RTI	−85.6	86.5	−179.8	−174.1	none	none	none
1RT1	−104.6	111.2	177.4	−145.6	none	none	none
1HNV	−66.5	123.8	−179	169.6	none	none	none
1VRT	−85.4	122.6	179.8	−167.3	none	none	none
1VRU	−94.0	116.8	179.8	164.3	none	none	none
1BQM	−76.3	95.2	177.8	−169.6	none	none	none
1FK9	−91.3	128.4	−178.6	−167.7	none	none	none
*Met*184							
1DLO	60.5	−160.6	179.2	−55.6	−179.3	−43.3	none
1RTD	58.3	−106.0	179.7	−84.2	−79.0	−148.5	none
1RTI	57.6	−117.0	−179.5	−70.8	178.2	−142.3	none
1RT1	55.0	−122.7	−178.9	−125.9	80.9	−109.4	none
1HNV	–	−100.1	174.5	−69.3	−86.1	−32.0	none
1VRT	53.8	−103.9	−177.4	−81.3	166.8	−152.8	none
1VRU	62.6	−116.4	−179.1	−90.7	169.1	116.9	none
1BQM	57.6	−83.8	−179.0	−56.5	−175.9	151.3	none
1FK9	51.6	−128.1	−179.9	−56.3	−146.5	−103.9	none
*Asp*185							
1DLO	−78.7	25.9	177.7	51.6	none	none	none
1RTD	−115.8	−0.3	−179.8	64.7	none	none	none
1RTI	−85.8	−13.3	−179.7	66.6	none	none	none
1RT1	−106.0	25.2	−179.1	−48.8	none	none	none
1HNV	−131.4	48.9	178.1	54.7	none	none	none
1VRT	−92.3	−12.7	−177.8	−123.3	none	none	none
1VRU	−88.7	−18.3	−175.6	−70.0	none	none	none
1BQM	−130.0	32.4	179.9	−53.1	none	none	none
1FK9	−90.0	10.5	179.7	−89.2	none	none	none
*Asp*186							
1DLO	−105.0	100.2	−179.7	−76.8	none	none	none
1RTD	−89.0	104.4	179.6	−149.0	none	none	none
1RTI	−90.9	131.5	179.8	−68.6	none	none	none
1RT1	−122.8	158.1	177.6	−66.3	none	none	none
1HNV	−135.2	135.3	−178.4	−91.6	none	none	none
1VRT	−102.4	162.3	178.7	−54.7	none	none	none
1VRU	−88.5	160.0	179.1	−54.9	none	none	none
1BQM	−134.8	149.1	178.7	−88.8	none	none	none
1FK9	−106.3	157.7	−179.4	−79.5	none	none	none

[a] Φ backbone torsion angle defined by the 4 atoms, $C_{(i-1)}$, $N_{(i)}$, $C_{\alpha(i)}$, $C_{(i)}$; φ backbone torsion angle defined by the 4 atoms, $N_{(i)}$, $C_{\alpha(i)}$, $C_{(i),}$ $N_{(i+1)}$; ω backbone torsion angle defined by the 4 atoms, $C_{\alpha(i)}$, $C_{(i)}$, $N_{(i+1)}$, $C_{\alpha(i+1)}$; χ_1 side chain torsion angle defined by the 4 atoms, $N_{(i)}$, $C_{\alpha(i)}$, $C_{\beta(i)}$, $C_{\gamma(i)}$; χ_2 side chain torsion angle defined by the 4 atoms, $C_{\alpha(i)}$, $C_{\beta(i)}$, $C_{\gamma(i)}$, $C_{\delta(i)}$; χ_3 side chain torsion angle defined by the 4 atoms, $C_{\beta(i)}$, $C_{\gamma(i)}$, $C_{\delta(i)}$, $C_{\varepsilon(i)}$; χ_4 side chain torsion angle defined by the 4 atoms, $C_{\gamma(i)}$, $C_{\delta(i)}$, $C_{\varepsilon(i)}$, $C_{\xi(i)}$; where i refers to the residue number

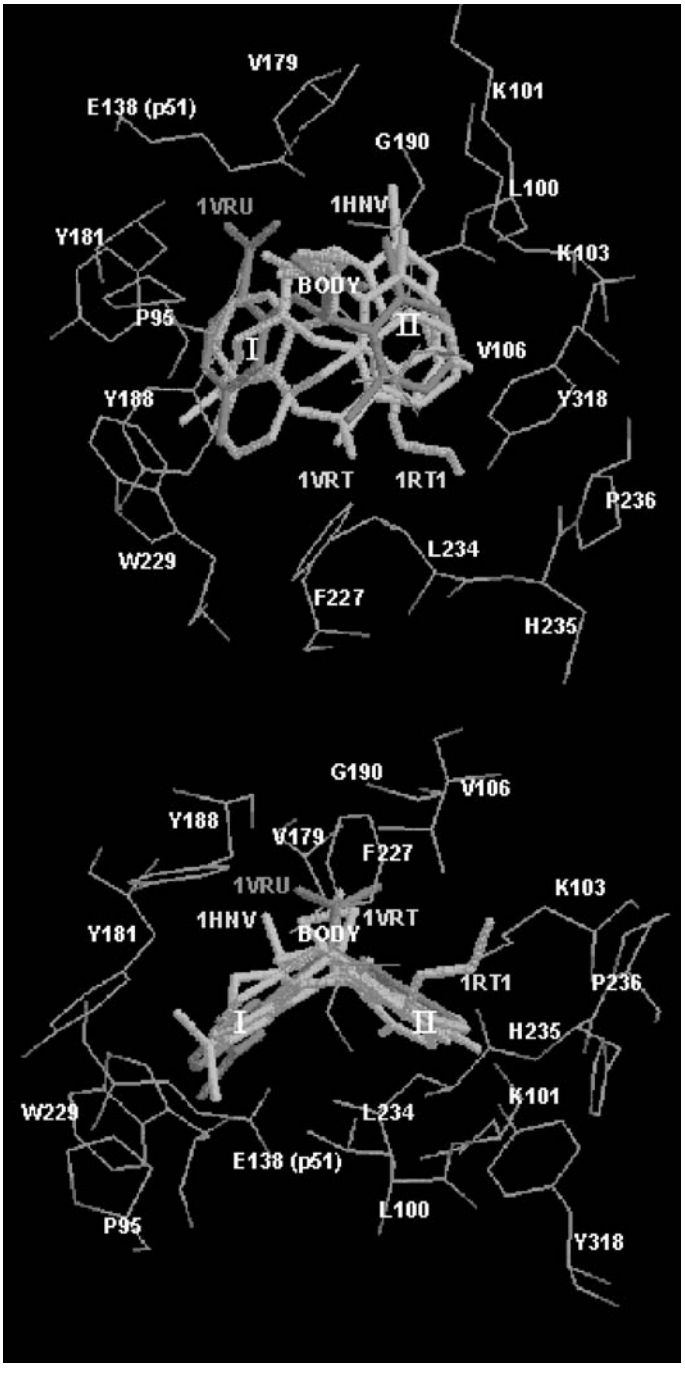

Fig. 2. Superposition of four structures of NNIs overlayed in the binding pocket; MKC-442 (1RT1), 8-Cl *TIBO* (1HNV), Nevirapine (1VRT), and 2,6-Cl_2 α-*APA* (1VRU)

The notion of a butterfly like shape of the inhibitor gets less stringent in case of the more recent NNIs called second generation inhibitors. Nevertheless there is still great similarity in shape and charge distribution. This global similarity of the NNIs

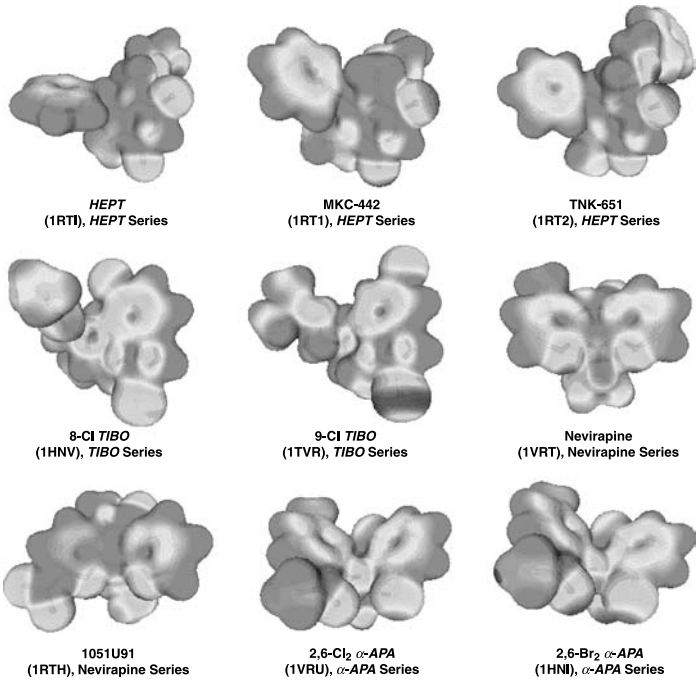

Fig. 3. Electrostatic potentials of NNIs, white indicate negatively charged parts of the molecules, positively charged parts are displayed in grey; hydrogen atoms are omitted from the models for reasons of clarity

is further exemplified by looking at the electrostatic potential of some of these compounds calculated with quantum chemical methods (see methods for calculation), which is presented in Fig. 3. As expected, these potentials show great similarity in corresponding regions of the molecules.

On NNI binding conformational reorientation of a great number of residues compared to free RT is observed. Especially large movements of the aromatic side chains of *Tyr*181 and *Tyr*188 can be seen. Only in the case of *HEPT* binding, the aromatic ring of *Tyr*181 remains in its original conformation. This is nicely demonstrated in Table 2 looking at the value of χ_1 for *Tyr*181 (PDB code 1RTI, -80 degrees compared to about 180 degrees in all other 44 NNI bound structures). Furthermore, the relative orientation of wing I and wing II of NNIs is also different in *HEPT* compared to all other NNIs. This might explain the relative weak binding affinity of *HEPT*. Especially in the case of strong inhibitors hydrogen bonds between the inhibitor and the main chain oxygen of *Lys*101 stabilise the structure of the complex. In the case of nevirapine (1VRT), a water molecule forms hydrogen bonds to both nevirapine and to the carbonyl oxygen of *Leu*234. Table 2 can also be used to validate earlier assumptions concerning common structural features of HIV-1 RT complexes. *Met*184 was mentioned to have an unusual conformation, which is stabilised by a hydrogen bond to *Gln*182. Looking at the complete list of backbone dihedral angles one can see that this is only true in 26 out of 44 cases. This is demonstrated more clearly in Table 3 where possible hydrogen bonds between *Met*184 and *Gln*182 or *Gln*161 are listed.

Table 3. The possible hydrogen bonds between *Met*184 and *Gln*182 or *Gln*161

PDB				Distance (Å)
RT-NNI				
1RT2	182	O	NE2	3.20
1JLA	182	O	NE2	2.69
1JLQ	182	O	NE2	2.82
1HNV	182	O	NE2	3.66
1TVR	182	O	NE2	2.96
1REV	182	O	NE2	3.94
1VRT	182	O	NE2	2.97
1FKP	182	O	NE2	2.80
1JLB	182	O	NE2	3.82
1RTH	182	O	NE2	3.01
1VRU	182	O	NE2	2.85
1HNI	182	O	NE2	3.57
1BQM	182	O	NE2	3.92
1KLM	182	O	NE2	2.89
1RT5	182	O	NE2	3.16
1RT7	182	O	NE2	2.88
1RT4	182	O	NE2	3.25
1C0U	182	O	NE2	3.51
1JLC	182	O	NE2	3.55
1EET	161	O	NE2	3.15
1IKY	161	O	NE2	2.93
1IKX	161	O	NE2	3.23
1FK9	161	N	OE1	3.48
1IKW	161	O	NE2	2.62
1FKO	161	N	OE1	3.34
1IKV	161	O	NE2	3.21
RT free				
1HMV	182	O	NE2	3.27
1RTJ	161	O	NE2	3.23
1DLO	182	O	NE2	3.07
1HQE	182	O	NE2	3.07
1JLE	161	O	NE2	3.50
1QE1	182	O	NE2	3.14

Distance greater 4 Å: **RT-NNI**: 1RTI, 1RT1, 1C1B, 1C1C, 1UWB, 3HVT, 1JLF, 1RT3, 1BQN, 1HPZ, 1HQU, 1RT6, 1JLG, 1C0T, 1DTT, 1DTQ, 1JKH, 1EP4; **RT-*RNA*/*DNA***: 2HMI, 1C9R, 1RTD, 1HYS

Functional groups of the NNIs used for superposition, which occupy the same space as the 5-substituent of the *HEPT* analogues are the 5*S*-methyl group of 8- and 9-chloro-*TIBO* the cyclopropyl group of nevirapine, the ethyl group of 1051U91, and the amide group of 2,6-dichloro-α-*APA* and 2,6-dibromo-α-*APA*. Another important point is the variable position of the two loops around *Pro*225 and *Pro*236, which are interacting with the different substituents of the 1-position of the inhibitors. These residues can adopt very different positions in order to maximize their interaction with different inhibitors. A shift as large as 5 Å has been observed

for the Cγ atom of *Pro*236 [16]. The movement of *Pro*236 is also responsible for the difference in volume of the binding pocket observed for various inhibitors.

In summary, three main points are important for efficient inhibitor binding to HIV-1 RT: 1) Burial of hydrophobic surface areas of the inhibitor, 2) The inhibitor should fit into its binding pocket as closely as possible, and 3) The ability of the inhibitor to form hydrogen bonds to the backbone of the protein. This is the combined result from numerous crystallographic studies of HIV-1 RT NNI complexes, which have been made available to the public in the last few years (Table 2 in Ref. [3]).

A more detailed understanding of the inhibition mechanism requires the examination of a series of chemically related compounds but preferentially with great variation in their potency. Five structures with inhibitors of the *HEPT* series are available and have been studied extensively [13, 16, 17] (PDB code 1RTI, 1RT1, 1RT2, 1C1B, 1C1C; see Fig. 1 in Ref. [3]). The surprisingly large difference of IC_{50} values for these compounds can be rationalized by comparing the different structures (*HEPT* 17 m*M*, MKC-442 8 n*M*, TNK-651 6 n*M*, GCA-186 2 n*M*, TNK-6123 6 n*M*). Several small conformational changes can be seen in the different complexes. The conformational switch already mentioned of Tyr181 of about 100 degrees going from *HEPT* to any other compound leads to an improved interaction of the inhibitors with the enzyme. The same is true for changing the methyl group in position 5 of the pyrimidine ring in *HEPT* to isopropyl in MKC-442 and TNK-651, which also leads to a significant increase in potency. The importance of the substituent at the 5-position of the pyrimidine ring on the biological activity of *HEPT* analogues was also shown in previous QSAR and CoMFA studies [18–21]. The structures of a second series of four related compounds (carboxanilide derivatives, PDB code 1RT4, 1RT5, 1RT6, 1RT7) have been published by *Ren et al*. [22].

Drug Resistance

One severe drawback of NNIs is the fast emergence of resistance mutants within days or weeks. Virus strains with reduced susceptibility to inhibitors are easily selected for. Moreover, these mutations very often also show decreased sensitivity to other RT inhibitors (cross resistance). Especially first generation NNIs like nevirapine and TNK-651 show a large decrease in binding affinity as a result of many different single point mutations in RT. These mutations are predominantly clustered around the binding site of the inhibitor pocket. Since the NNI binding pocket is different from the active site many mutations in the NNI binding pocket still result in a functional enzyme. More recently compounds have been found which have a more favourable resistance profile [23]. These so-called second generation NNIs require more than one mutation to turn the enzyme to be resistant against the inhibitor.

Resistance mutations are found for many residues, which are in close contact to the inhibitor. An example is the side chain of *Val*106, which in most cases has extensive *Van der Waals* contacts to the inhibitor (see Table 1). These interactions might be lost on mutation to *Ala*. The same argument holds for *Leu*100*Ile*. Also the mutation *Tyr*181*Cys* causes high resistance against many NNIs [13]. As the crystal structure of the mutant RT in complex with 8-Cl *TIBO* [24] (1UWB) is known, this resistance can be explained by the loss of interaction between the inhibitor and the aromatic side chain of *Tyr*181. Two wild type structures have been reported where

the phenyl group of the inhibitor interacting with *Tyr*181 was either modified (GCA-186) or replaced by a cyclohexyl group (TNK-6123) [17]. Both compounds are reported to have significantly improved potency in the case of a *Tyr*181*Cys* mutation. For TNK-6123 this was explained with a greater flexibility of the cyclohexyl ring to compensate the loss of aromatic interaction. Similar effects have been observed for the mutation *Tyr*188*Leu* complexed with HBY 097 [25]. Furthermore, in this structure *Leu*188 can adopt many different conformations leading to short contact distances to the inhibitor. This idea is strengthened by the fact that *Leu*188 has no clear electron density in p66 [25]. The same effect has been observed in the *Tyr*181*Cys* mutant with inhibitor R86183 [24]. In a recent study, however, the structures of *Tyr*181*Cys* and *Tyr*188*Cys* mutants with various inhibitors were described [26]. In all cases a well defined electron density was observed at position 181 and 188. Therefore, the loss of aromatic interaction in first generation compounds is thought to be the main reason for weaker drug binding. This aromatic interaction is of much less importance in the case of second generation NNIs, which leads to a better resistance profile at least for mutations at positions 181 and 188. Another frequently observed mutation is *Pro*236*Leu*, which increases the backbone flexibility, thereby allowing more favourable *Van der Waals* interactions with the inhibitor. The *Lys*103*Asn* mutation of RT was studied with and without inhibitors [27, 11]. *Lys*103 is located at the entrance of the pocket. In one study the inhibitors HBY 097 and R90385 were used [11]. The binding mode of inhibitors bound to wild-type or the *Lys*103*Asn* mutant show similar interactions with the inhibitor. The different binding affinities are explained by the formation of an extra hydrogen bond between the side-chain nitrogen of *Asn*103 and *Tyr*188 in free RT (closed conformation). This hydrogen bond is not possible in the wild-type. Interestingly this hydrogen bond has already been postulated by *Esnouf et al*. in 1995, based on their structure of free RT [28]. In a second study nevirapine and the second generation inhibitor efavirenz were used [27]. With efavirenz a reorientation of the NNI binding pocket with repositioning of the inhibitor was observed. The aromatic ring of residue 181 remains in the wild type position. These different rearrangements might be responsible for the better resilience to drug resistance mutation of efavirenz compared to nevirapine.

Other mutation reported from *in vivo* and *in vitro* studies are *Lys*101*Glu*/*Asp* where positive charges are changed to negative ones. The reverse is true for *Glu*138*Lys*, while in *Val*179*Asp*/*Glu* and *Gly*190*Glu* there is an increase of negative charge. For a more complete understanding of these mutations further structural investigations are necessary.

Conclusion

This quantitative study of known structures of RT and its complexes with inhibitors supports many details about conformational changes and rearrangements of subdomains, which have been published by various groups in the last few years. In addition it leads to a more detailed understanding of the importance of distinct amino acid residues in the NNI binding site. For instance residue *Trp*229 is in close contact to all NNIs (Table 1). A large overall displacement is observed on NNI binding with small local conformational changes only [3]. However, no escape

mutants of this amino acid are observed because this leads to a severe decrease of the enzymes activity in the absence of any inhibitor. As another example we mention the turn around *Met*184. It shows different conformation in various inhibitor complexes. This can be seen from the variety of possible forms of hydrogen bonding to their residue (Table 1). Another example is the conformation of *Tyr*181. A pronounced flip of the aromatic ring is observed in all cases of NNI binding, except for *HEPT*. Only in this case it remains in the free enzyme conformation. For a complete understanding of the inhibition mechanism of HIV-1 RT the detailed knowledge of the conformations of the amino acid residues involved is necessary. To this end the determination of more structures will be necessary, especially of mutant type enzyme complexes.

Methods

The following software packages were used: SYBYL 6.5 [29] for the visualisation of the structures, GAUSSIAN 94 [30] for the electron density calculations, and gOpenMol 1.3.1 [31] for the presentation of the electrostatic potentials (ESP). Tsar [32] calculated molecular properties of NNIs. TINKER 3.6 [33] using the AMBER force field [34] did the superpositions of the molecules.

Acknowledgements

This work was supported by grants from the Thailand Research Fund (TRF) project MRG4680111. *S. Hannongbua* is grateful to TRF and KURDI for research fellowship (RSA4480001). The quantum chemical calculations were performed on the Cluster of Digital Alpha Servers (2100 4/275) of the computer centre of the University of Vienna. Generous supply of computer time on this installation is grateful acknowledged. The authors thank *S. Maurer-Stroh* for carefully reading the manuscript.

References

[1] Re MC, Monari P, Bon I, Boderi M, Gibellini D, Schiavone P, Vitone F, Furlini G, La Placa M (2002) Int J Antimicrob Agents **20**: 223
[2] De Clercq E (1999) Il Farmaco **54**: 26
[3] Lawtrakul L, Beyer A, Hannongbua S, Wolschann P (2004) Monatsh Chem, in press
[4] Miyasaka T, Tanaka H, Baba M, Hayakawa H, Walker RT, Balzarini J, De Clercq E (1989) J Med Chem **32**: 2507
[5] Debyser Z, Pauwels R, Andries K, Desmyter J, Kukla MJ, Janssen PAJ, De Clercq E (1991) Proc Natl Acad Sci USA **88**: 1451
[6] Merluzzi VJ, Hargrave KD, Labadia M, Grozinger K, Skoog M, Wu JC, Shih C-K, Eckner K, Hattox S, Adams J, Rosehthal AS, Faanes R, Eckner RJ, Karp RA, Sullivan JL (1990) Science **250**: 1411
[7] Goldman ME, Nunberg JH, O'Brien JA, Quintero JC, Schleif WA, Freund KF, Gaul SL, Saari WS, Wal JS, Hoffman JM, Anderson PS, Hupe DJ, Emini EA, Stern AM (1991) Proc Natl Acad Sci USA **88**: 6863
[8] Romero DL, Busso M, Tan CK, Reusser F, Palmer JR, Poppe SM, Aristoff PA, Downey KM, So AG, Resnick L, Tarpley WG (1991) Proc Natl Acad Sci USA **88**: 8806
[9] Balzarin J, Pérez-Pérez M-J, San-Felix A, Schols D, Perno CF, Vandamme AM, Camarasa MJ, De Clercq E (1992) Proc Natl Acad Sci USA **89**: 4392

[10] Pauwels R, Andries K, Debyser Z, Van Daele P, Schols D, Stoffels P, De Vreese K, Woestenborghs R, Vandamme AM, Janssen CGM, Anne J, Cauwenbergh G, Desmyter J, Heykant J, Janseen MAC, De Clercq E, Janssen PAJ (1993) Proc Natl Acad Sci USA **90**: 1711
[11] Hsiou Y, Ding J, Das K, Clark AD, Boyer PL, Lewi P, Janssen PAJ, Kleim J-P, Roesner M, Hughes SH, Arnold E (2001) J Mol Biol **309**: 437
[12] Kohlstaedt LA, Wang J, Friedman JM, Rice PA, Steitz TA (1992) Science **256**: 1783
[13] Ren J, Esnouf R, Garman E, Somers D, Ross C, Kirby I, Keeling J, Darby G, Jones Y, Stuart D, Stammers D (1995) Nat Struct Biol **2**: 293
[14] Jacobo-Molina A, Ding J, Nanni RG, Clark AD, Lu X, Tantillo Ch, Williams RL, Kamer G, Ferris AL, Clrak P, Hizi A, Hughes SH, Arnold E (1993) Proc Natl Acad Sci USA **90**: 6320
[15] Ding J, Das K, Moereels H, Koymans L, Andries K, Janssen PA, Hughes SH, Arnold E (1995) Nat Struct Biol **2**: 407
[16] Hopkins AL, Ren J, Esnouf RM, Willcox BE, Jones EY, Ross C, Miyasaka T, Walker RT, Tanaka H, Stammers DK, Stuart DI (1996) J Med Chem **39**: 1589
[17] Hopkins AL, Ren J, Tanaka H, Baba B, Okamato M, Stuart DI, Stammers DK (1999) J Med Chem **42**: 4500
[18] Hannongbua S, Lawtrakul L, Limtrakul J (1996) J Comput Aided Mol Des **10**: 145
[19] Hannongbua S, Lawtrakul L, Sotriffer CA, Rode BM (1996) Quant Struct-Act Relat **15**: 389
[20] Lawtrakul L, Hannongbua S (1999) Sci Pharm **67**: 43
[21] Pungpo P, Hannongbua S, Wolschann P (2003) Curr Med Chem **10**: 1661
[22] Ren J, Esnouf RM, Hopkins AL, Warren J, Balzarini J, Stuart DI, Stammers DK (1998) Biochemistry **37**: 14394
[23] De Clercq E (1998) Antiviral Res **38**: 153
[24] Das K, Ding J, Hsiou Y, Clark AD Jr, Moereels H, Koymans L, Andries K, Pauwels R, Janssen PAJ, Boyer PL, Clark P, Smith RH Jr, Smith MBK, Michejda CJ, Hughes SH, Arnold E (1996) J Mol Biol **264**: 1085
[25] Hsiou Y, Das K, Ding J, Clark AD Jr, Kleim JP, Rosner M, Winkler I, Riess G, Hughes SH, Arnold E (1998) J Mol Biol **284**: 313
[26] Ren J, Nichols C, Bird L, Chamberlain P, Weaver K, Short S, Stuart DI, Stammer DK (2001) J Mol Biol **312**: 795
[27] Ren J, Milton J, Weaver KL, Short SA, Stuart DI, Stammers DK (2000) Structure **8**: 1089
[28] Esnouf R, Ren J, Ross C, Jones Y, Stammers D, Stuart D (1995) Nat Struct Biol **2**: 303
[29] Tripos Associates, Inc (1996) SYBYL Molecular Modelling Software, Version 6.5. St. Louis, MO
[30] Frisch MJ, Trucks GW, Schlegel HB, Gill PMW, Johnson BG, Robb MA, Cheeseman JR, Keith T, Petersson GA, Montgomery JA, Raghavachari K, Al-Laham MA, Zakrzewski VG, Ortiz JV, Foresman JB, Peng CY, Ayala PY, Chen W, Wong MW, Andres JL, Replogle ES, Gomperts R, Martin RL, Fox DJ, Binkley JS, Defrees DJ, Baker J, Stewart JP, Head-Gordon M, Gonzales C, Pople JA (1995) Gaussian 94 (Version B 3); Gaussian Inc., Pittsburgh, PA
[31] Laaksonen L (1999) User's manual for gOpenMol. Espoo, Finland
[32] Oxford Molecular Ltd. (1997) Tsar 3.1 User guide. England
[33] Jay Ponder Lab, Dept. of Biochemistry & Molecular Biophysics; Washington University School of Medicine (1998) TINKER-Software Tools for Molecular Design. St. Louis, Missouri
[34] Weiner SJ, Kollman PA, Case DA, Singh UC, Ghio C, Alagona G, Profeta S, Weiner P (1984) J Am Chem Soc **106**: 765

Verleger: Springer-Verlag GmbH, Sachsenplatz 4–6, 1201 Wien, Austria. – Herausgeber: Österreichische Akademie der Wissenschaften, Dr.-Ignaz-Seipel-Platz 2, 1010 Wien, und Gesellschaft Österreichischer Chemiker, Eschenbachgasse 9, 1010 Wien, Austria. – Redaktion: Getreidemarkt 9/163-OC, 1060 Wien, Austria. – Satz und Umbruch: Thomson Press Ltd., Chennai, India. – Offsetdruck: Manz Crossmedia, 1051 Wien, Austria. – Verlagsort: Wien. – Herstellungsort: Wien. – Printed in Austria.